Mean first passage times across a potential barrier in the lumped state approximation

Eric J. Mapes and Mark F. Schumaker
Department of Pure and Applied Mathematics, Washington State University, Pullman, Washington 99164-3113

(Received 30 June 2000; accepted 12 October 2000)

The lumped state approximation (LSA) is a method for handling boundary conditions for diffusion on an interval which simplifies the description of transitions into and out of the interval. It was originally motivated by the problem of proton conduction through the ion channel gramicidin. This paper discusses the mean first passage time of a diffuser crossing a potential barrier in the lumped state approximation. The LSA mean first passage time is shown to be identical to a different quantity, the interior mean first passage time, clarifying the nature of the approximation. We also discuss a variant of the LSA in which dependence on an applied electrical potential is made explicit; an optimal value for an effective electrical distance is found. A detailed comparison is made of the LSA mean first passage time with several other formulations of the mean time to cross a barrier. [DOI: 10.1063/1.1330215]

I. INTRODUCTION

This paper describes the lumped state approximation (LSA), a method for handling boundary conditions for diffusion on an interval which simplifies the description of transitions into and out of the interval. The first section describes the problem which motivated the introduction of this method, namely the mechanism of proton conduction through the ion channel gramicidin. References 1 and 2 introduced the LSA in order to make this problem analytically soluble. The next section discusses the derivation of the differential equation for the mean first passage time to diffuse across an interval with boundary conditions incorporating the LSA. This mean time is then compared with an *exact* time to cross the barrier (the mean time to cross from the potential minimum on one side to the minimum on the other) and an *interior* mean time that is closely related to the exact time. The LSA mean first passage time is shown to be identical to the interior mean first passage time, making it easy to characterize the difference between the LSA and exact mean first passage times. We also analyze an effective electrical distance (EED) variant of the LSA in which dependence on an applied electrical potential is made explicit. This was used in the analysis of proton conduction. Below, we find a formula for the optimal effective electrical distance. In the numerical computations section, these different ways of computing the mean first passage time to cross a barrier are compared with each other and Kramers's escape rate theory.[3]

A. The proton conduction model

Gramicidin A is a linear pentadecapeptide consisting of alternating L and D amino acids. The ion conducting conformation in membranes has been established by nuclear magnetic resonance.[4–6] An N-terminal to N-terminal dimer is formed by two single-stranded right-handed β-helices whose axes are oriented perpendicular to the plane of the membrane. The pore of the dimer has the dimensions of approximately ten water molecules in single file.

Pomès and Roux have carried out molecular dynamics simulations of gramicidin with[7,8] and without[8] a single excess proton. From these simulations, potentials of mean force are calculated as a function of the reaction coordinates, which are proportional to the axial components of the dipole moments of the pore contents. References 1 and 2 obtain diffusion coefficients for these reaction coordinates from their velocity autocorrelation functions. They then construct a *framework* model, designed to incorporate the information from molecular dynamics and use it to calculate conductances which are compared with experiment.

Figure 1(A) sketches a simplified configuration space for proton conduction through gramicidin, as described by the framework model. The top or proton segment represents the domain of a reaction coordinate which follows the progress of the center of excess charge through the pore from side I to side II. The bottom or reorientation segment represents the domain of a reaction coordinate which follows the reorientation of water molecules in an *empty* pore, that is, one without an excess proton. In the empty pore, waters tend to be close to one of the two idealized configurations with the axial components of the dipole moments aligned. A useful simplification is to imagine that there is a defect in the packing of pore waters about which the axial components of the water dipole moments turn. Reorientation of the pore waters can then be visualized as due to the diffusion of the defect from one end of the column to the other.

Consider a trajectory around the cycle in Fig. 1(A). For example, suppose an excess proton enters the pore on side I and exits on side II. Immediately after the proton leaves the pore, the water column may be left in a range of orientations. These can be visualized by supposing the defect could be located anywhere in a boundary region near one end of the

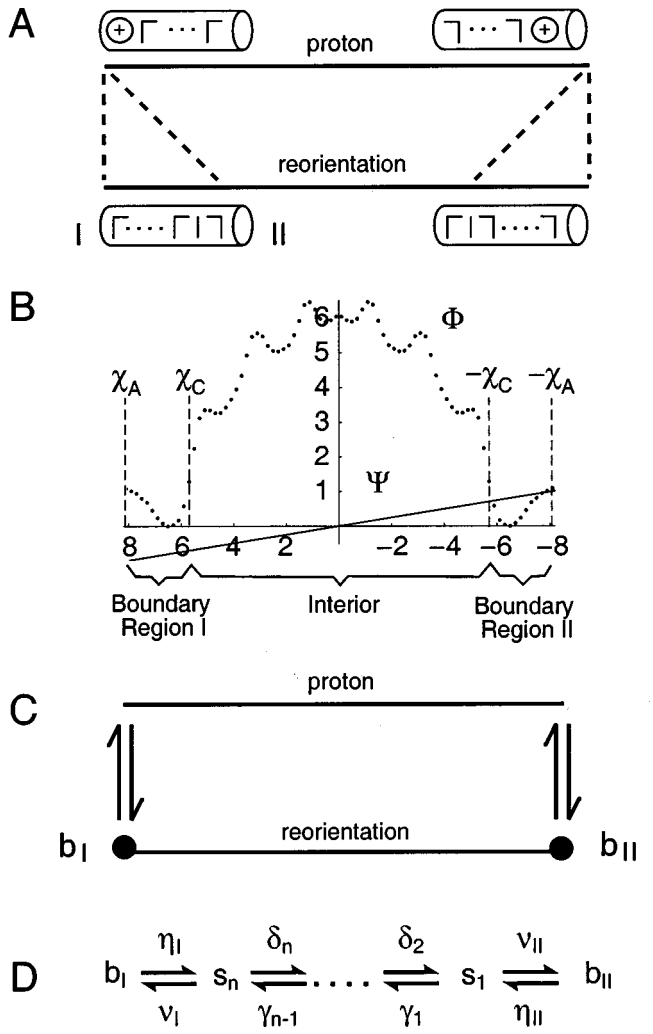

FIG. 1. (A) A sketch of a simplified configuration space for proton conduction through gramicidin. Cartoons sketch the configuration of pore waters near the ends of the proton and reorientation segments. The cartoon at the lower left hand corner also shows side I and side II of the channel. (B) Reorientation potentials of mean force Φ (dots) and the applied potential energy Ψ (line). For the example shown, $\chi_C = 5.7\ e_0$ Å and $\chi_A = 8.1\ e_0$ Å. The reaction coordinate of the simulations, χ, is rescaled to the axial component of the dipole moment of the pore content, μ, by $\mu = \alpha\chi$, where $\alpha \approx 0.435$. (C) State diagram of proton conduction mechanism with the boundary regions lumped into discrete points. (D) The random walk model used to construct the lumped state approximation.

channel: near side I for the defect sketched in the figure. If pore waters then rotate to reverse the dipole moment of the pore contents, the electrostatic interaction will again favor proton entry on side I. The defect must cross the pore interior to reverse the dipole moments. When it is located in a boundary region on the other side of the channel, another proton can enter on side I. Possible transitions between the proton and reorientation segments are suggested by the two pairs of dashed lines. The reorientation segment is thus divided into three regions: boundary regions I and II where transitions to and from the proton segment can be made, and the interior of the reorientation segment, between the boundary regions.

The abscissa of Fig. 1(B) is the orientation moment of the pore contents χ, the reaction coordinate of the molecular dynamics simulations. This quantity is defined by the formal charges of the water molecules used in the simulations.[1] χ is rescaled to give μ, the axial component of the dipole moment of the pore contents. The scaling is given by $\mu = \alpha\chi$, where $\alpha \approx 0.435$ assumes that pore water dipole moments have magnitude 0.5 e_0 Å, within the range of estimates given by Duca and Jordan.[9] The axial component of the pore dipole moment is negative in the lower right hand cartoon of Fig. 1(A) and positive in the lower left hand cartoon. Correspondingly, the abscissa of Fig. 1(B) advances from right to left.

The units of the ordinate of Fig. 1(B) are energy, given in $k_B T$, where $T = 298$ K. The figure shows the *intrinsic* potential of mean force for water reorientation,[1,8] Φ, and the potential energy due to an applied transmembrane potential, Ψ, as a function of χ. The word intrinsic refers to all components of the potential apart from the transmembrane potential. In principle, this includes both short range interactions between the water column and the channel as well as longer range interactions between the column and channel environment. However, the simulations only included the channel, the pore waters, and a few waters clustered about each channel entrance. The simulations give estimates of Φ at $\chi = -8.1, -7.9, -7.7, \ldots, 7.9, 8.1\ e_0$ Å. Linear interpolation between these points completes the definition. The maximum extent of the reorientation segment is defined by $\mu = \pm\mu_A$, and the maximum extent of the interior region is defined by $\mu = \pm\mu_C$. The corresponding values χ_A and χ_C are shown in Fig. 1(B). The interior region corresponds to the broad central barrier of Φ and the boundary regions to the potential minima on either side. An applied potential is assumed to give rise to a constant field in the pore; this is a good approximation due to the cylindrical geometry of the channel.[10,11] Consequently, Ψ is linear. The slope shown in Fig. 1(B) corresponds to a positive applied potential of $V_{\mathrm{I}} = 167$ mV on side I, with $V_{\mathrm{II}} = 0$ by convention. We consider Φ and Ψ to be functions of μ. The total potential energy is $W(\mu) = \Phi(\mu) + \Psi(\mu)$.

Intuitively, it seems reasonable that diffusion through the narrow pore of gramicidin has a quasi-one-dimensional character. However, an attempt to construct a permeation theory of single proton conduction through gramicidin by scaling transitions directly between the endpoints of the proton and reorientation segments of Fig. 1(A) does not produce a satisfactory result.[12] Instead, it is necessary to assume that transitions are possible to and from intervals on the reorientation segment—the boundary regions. With two continuous sets of transitions between the proton and reorientation segments, the dynamics of the single proton model would no longer be strictly one-dimensional. The LSA assumes that these regions of higher-dimensional dynamics are localized near the channel entrances. Transitions are then simplified by lumping the boundary region between $-\mu_A$ and $-\mu_C$ into a single point, the boundary state b_{II}, and the boundary region between μ_C and μ_A into the boundary state b_{I}. Figure 1(C) shows the state diagram of the resulting proton conduction model. Instead of a continuum of possible transitions between the two segments, there is only a single transition at each end. This allows the proton conduction model to be solved analytically.

II. LSA MEAN FIRST PASSAGE TIMES

Figure 1(D) represents the random walk model used to construct the lumped state approximation of the mean first passage time. This will ultimately result in a diffusion process describing Brownian motion of the reorientation reaction coordinate. Note that the indices in Fig. 1(D) progress from right to left, corresponding to the orientation of the abscissa of Fig. 1(B). The *boundary states* b_{I} and b_{II} represent the boundary regions discretized by the LSA. States s_i, $1 \leqslant i \leqslant n$, are the domain of the random walk between b_{I} and b_{II}. Each state corresponds to a subinterval of the interior region of the reorientation segment of width $\Delta\mathcal{L}=\mathcal{L}/n$, where $\mathcal{L}=2\mu_C$ is the width of the interior region. We denote by μ_i the dipole moment associated with state s_i. Time is also discrete, with constant time step Δt. At each time step and for $1 \leqslant i \leqslant n$, γ_i is the forward transition probability from state s_i to state s_{i+1}, and δ_i is the backward transition probability from state s_i to state s_{i-1}. Let R represent either I or II. Then η_R is the transition probability of entering the interior region of the reorientation segment from boundary state b_R, and v_R is the transition probability of leaving the interior region to enter state b_R.

A. Differential equation

A differential equation will be developed for the mean time before a diffuser, starting at reaction coordinate $\mu \in [-\mu_C, \mu_C]$, first reaches state b_I at $\mu=\mu_C$. Consider the system initially at site s_i where $2 \leqslant i \leqslant n-1$, $t=t_0$. If $Q_j(t)$ is the probability that site s_j is occupied at time t, then $Q_j(t_0)=\delta_{ij}$. The probability that the diffuser stays at site i after a time step is $Q_i(t_0+\Delta t)=1-\gamma_i-\delta_i$. The probability that the diffuser moves forward is $Q_{i+1}(t_0+\Delta t)=\gamma_i$ and backward is $Q_{i-1}(t_0+\Delta t)=\delta_i$. Let $\overline{t_i}$ be the mean time before a diffuser, starting at site s_i, escapes to b_I. After one time step, express the mean first passage time before absorption as a weighted average:

$$\overline{t_i}-\Delta t = Q_i(t_0+\Delta t)\overline{t_i} + Q_{i+1}(t_0+\Delta t)\overline{t_{i+1}} + Q_{i-1}(t_0+\Delta t)\overline{t_{i-1}}. \tag{1}$$

Substituting in the expressions for the Q_i in terms of transition probabilities yields

$$-\Delta t = -(\gamma_i+\delta_i)\overline{t_i} + \gamma_i\overline{t_{i+1}} + \delta_i\overline{t_{i-1}}. \tag{2}$$

Transition probabilities are defined to satisfy the Boltzmann distribution

$$P(\mu) = Ke^{-\beta W(\mu)} \tag{3}$$

at equilibrium, where $P(\mu)$ is the probability density on the reorientation segment and K is a constant. Let

$$\gamma_i = \Delta t\mathcal{D}(\Delta\mathcal{L})^{-2}\exp\{(\beta/2)[W(\mu_i)-W(\mu_{i+1})]\}, \tag{4}$$

$$\delta_i = \Delta t\mathcal{D}(\Delta\mathcal{L})^{-2}\exp\{(\beta/2)[W(\mu_i)-W(\mu_{i-1})]\}, \tag{5}$$

where $\beta=(k_BT)^{-1}$. $\mathcal{D}$ is the diffusion coefficient associated with the coordinate μ, with units of (dipole moment)^2/time. $\Delta\mathcal{L}=\mathcal{L}/n$ is the distance between states. The time step Δt is scaled with n so that γ_i and δ_i remain positive and finite as $n\to\infty$: $\Delta t=\Delta\tau/n^2$, where $\Delta\tau$ is independent of n.

The transition probabilities may be expanded in the small parameter n^{-1} to give a useful expression for large n. The expansion gives

$$\gamma_i = \Delta t\mathcal{D}(\Delta\mathcal{L})^{-2} \times[1-\beta\Delta\mathcal{L}W'(\mu_i)/2+(\Delta\mathcal{L})^2\epsilon_i+\mathcal{O}(n^{-3})], \tag{6}$$

$$\delta_i = \Delta t\mathcal{D}(\Delta\mathcal{L})^{-2} \times[1+\beta\Delta\mathcal{L}W'(\mu_i)/2+(\Delta\mathcal{L})^2\epsilon_i+\mathcal{O}(n^{-3})], \tag{7}$$

where

$$\epsilon_i = -\beta W''(\mu_i)/4+\beta^2W'(\mu_i)^2/8. \tag{8}$$

Substitute Eqs. (6) and (7) into Eq. (2), organize terms, and divide by $\Delta t\mathcal{D}$ to obtain

$$-\frac{1}{\mathcal{D}} = \frac{-2\overline{t_i}+\overline{t_{i+1}}+\overline{t_{i-1}}}{(\Delta\mathcal{L}^2)} + \frac{\beta W'(\mu_i)(\overline{t_{i-1}}-\overline{t_{i+1}})}{2\Delta\mathcal{L}} + \epsilon_i(-2\overline{t_i}+\overline{t_{i+1}}+\overline{t_{i-1}})+\mathcal{O}(n^{-1}). \tag{9}$$

Putting $\overline{t_i}=\overline{t}(\mu_i)$, we recognize the first two terms on the right hand side as first and second differences, respectively. The limit $n\to\infty$ then yields a differential equation for $\overline{t}(\mu)$:

$$-1=\mathcal{D}[\overline{t}''(\mu)-\beta W'(\mu)\overline{t}'(\mu)]. \tag{10}$$

This equation describes the evolution of the mean first passage time in the interior region of the reorientation segment.

B. Entrance and exit transition probabilities

We next find expressions for the entrance and exit transition probabilities η_R and ν_R. Under the condition of detailed balance we have

$$Q_{\mathrm{I}}^b/Q_n = \nu_{\mathrm{I}}/\eta_{\mathrm{I}}, \tag{11}$$

$$Q_{\mathrm{II}}^b/Q_1 = \nu_{\mathrm{II}}/\eta_{\mathrm{II}}, \tag{12}$$

where Q_{I}^b and Q_{II}^b are the probabilities of the boundary states. At equilibrium, these are given by

$$Q_{\mathrm{I}}^b = \int_{\mu_C}^{\mu_A} P(\mu')d\mu', \tag{13}$$

$$Q_{\mathrm{II}}^b = \int_{-\mu_A}^{-\mu_C} P(\mu')d\mu', \tag{14}$$

where $P(\mu)$ is given by Eq. (3). Note that $Q_i=P_i\Delta\mathcal{L}+\mathcal{O}(n^{-2})$, where $P_i=P(\mu_i)$. Substitute Eq. (13) into Eq. (11) and Eq. (14) into Eq. (12), use the Boltzmann distribution Eq. (3), and take the limit as $n\to\infty$ to obtain

$$\lim_{n\to\infty}\frac{\nu_{\mathrm{I}}}{n\eta_{\mathrm{I}}} = a_{\mathrm{I}}, \tag{15}$$

$$\lim_{n\to\infty}\frac{\nu_{\mathrm{II}}}{n\eta_{\mathrm{II}}} = a_{\mathrm{II}}, \tag{16}$$

where the boundary weights a_{I} and a_{II} are proportional to integrals over the Boltzmann distribution:

$$a_{\mathrm{I}}=\mathcal{L}^{-1}\int_{\mu_C}^{\mu_A} e^{-\beta\Delta W(\mu')}\,d\mu', \tag{17}$$

$$a_{\mathrm{II}}=\mathcal{L}^{-1}\int_{-\mu_A}^{-\mu_C} e^{-\beta\Delta W(\mu')}\,d\mu'. \tag{18}$$

We have introduced $\Delta W(\mu)=W(\mu)-W(\mu_0)$ where $\mu_0=\mu_C$ on side I and $\mu_0=-\mu_C$ on side II. The following definitions satisfy the constraints given by Eqs. (15) and (16):

$$\nu_{\mathrm{I}}=\Delta t(\mathcal{D}/\Delta\mathcal{L}^2)a_{\mathrm{I}}, \tag{19}$$

$$\nu_{\mathrm{II}}=\Delta t(\mathcal{D}/\Delta\mathcal{L}^2)a_{\mathrm{II}}, \tag{20}$$

$$\eta_{\mathrm{I}}=\eta_{\mathrm{II}}=\Delta t(\mathcal{D}/\Delta\mathcal{L}^2)n^{-1}. \tag{21}$$

The transition probabilities ν_{I} and ν_{II} scale with n in the same way as γ_i and δ_i. This is consistent with modeling transport from the interior to the boundary states as diffusive. The scaling of η_{I} and η_{II} with n is then determined by the requirement that detailed balance be satisfied at equilibrium. In particular, the boundary states retain positive probability in the limit $n\to\infty$.

C. Boundary conditions

Boundary conditions for $\overline{t}$ are developed at $\mu=-\mu_C$, on side II, the right side of the reorientation potential profile in Fig. 1(B), and at $\mu=\mu_C$, on side I, the left side of the reorientation potential profile in Fig. 1(B). Assume the diffuser starts at site $i=1$ at $t=t_0$. Thus $Q_1(t_0)=1$, $Q_j(t_0)=0$, for $j\neq 1$. The probability of forward movement is γ_1 and the probability of backward movement is ν_{II}. After one time step $Q_1(t_0+\Delta t)=1-\gamma_1-\nu_{\mathrm{II}}$, $Q_2(t_0+\Delta t)=\gamma_1$, and $Q_{\mathrm{II}}^b(t_0+\Delta t)=\nu_{\mathrm{II}}$. The mean time before reaching side I is initially $\overline{t}_1$ and after one time step it is $\overline{t}_1-\Delta t$. Expressing this as a weighted average

$$\overline{t}_1-\Delta t=Q_1(t_0+\Delta t)\overline{t}_1+Q_2(t_0+\Delta t)\overline{t}_2+Q_{\mathrm{II}}^b(t_0+\Delta t)\overline{t}_{\mathrm{II}} \tag{22}$$

and substituting for the Q's yields

$$-\Delta t=(-\gamma_1-\nu_{\mathrm{II}})\overline{t}_1+\gamma_1\overline{t}_2+\nu_{\mathrm{II}}\overline{t}_{\mathrm{II}}, \tag{23}$$

where $\overline{t}_{\mathrm{II}}$ is the mean time required for a diffuser starting at side II to escape to side I.

Next obtain an expression for $\overline{t}_{\mathrm{II}}$ by considering a mean first passage time problem which begins at state b_{II}. Let $Q_{\mathrm{II}}^b(t_0)=1$. After one time step, $Q_{\mathrm{II}}^b(t_0+\Delta t)=1-\eta_{\mathrm{II}}$ and $Q_1(t_0+\Delta t)=\eta_{\mathrm{II}}$. Hence the weighted average is

$$\overline{t}_{\mathrm{II}}-\Delta t=Q_{\mathrm{II}}^b(t_0+\Delta t)\overline{t}_{\mathrm{II}}+Q_1(t_0+\Delta t)\overline{t}_1. \tag{24}$$

The appropriate substitutions yield $\overline{t}_{\mathrm{II}}=\overline{t}_1+\Delta t/\eta_{\mathrm{II}}$. Using this value for $\overline{t}_{\mathrm{II}}$, Eq. (23) becomes

$$-\Delta t=\gamma_1(\overline{t}_2-\overline{t}_1)+(\nu_{\mathrm{II}}\Delta t)/\eta_{\mathrm{II}}. \tag{25}$$

Substituting from Eqs. (6), (20), and (21) for the transition probabilities yields

$$-\Delta\mathcal{L}/\mathcal{D}=(\overline{t}_2-\overline{t}_1)/\Delta\mathcal{L}+\mathcal{L}a_{\mathrm{II}}/\mathcal{D}+\beta W'(\mu_1)(\overline{t}_1-\overline{t}_2)/2+\Delta\mathcal{L}\epsilon_1(\overline{t}_2-\overline{t}_1)+\mathcal{O}(n^{-2}). \tag{26}$$

Now let $n\to\infty$, so that $\Delta\mathcal{L}\to 0$. All of the terms except the first two on the right side of Eq. (26) go to zero in this limit. Hence

$$\overline{t}'(-\mu_C)=-\mathcal{L}a_{\mathrm{II}}/\mathcal{D}. \tag{27}$$

Next consider the boundary condition for $\overline{t}$ on side I where $i=n$. Let $Q_n(t_0)=1$, $Q_j(t_0)=0$, for $j\neq n$. The probability of forward movement is ν_{I} and the probability of backward movement is δ_n. So $Q_n(t_0+\Delta t)=1-\nu_{\mathrm{I}}-\delta_n$, $Q_{n-1}(t_0+\Delta t)=\delta_n$, and $Q_{\mathrm{I}}^b(t_0+\Delta t)=\nu_{\mathrm{I}}$. Since $\overline{t}_{\mathrm{I}}=0$,

$$\overline{t}_n-\Delta t=Q_n(t_0+\Delta t)\overline{t}_n+Q_{n-1}(t_0+\Delta t)\overline{t}_{n-1}. \tag{28}$$

With the appropriate substitutions we get

$$-\Delta t=-\nu_{\mathrm{I}}\overline{t}_n+\delta_n(\overline{t}_{n-1}-\overline{t}_n). \tag{29}$$

Let $n\to\infty$ to find

$$\overline{t}(\mu_C)=0. \tag{30}$$

Side I is an absorbing boundary.

D. Solution

The LSA mean first passage time $\overline{t}_{\mathrm{LSA}}(\mu)$ is the solution of the differential equation (10) with boundary conditions Eqs. (27) and (30). Consider first the homogeneous equation $\overline{t}_h(\mu)$ corresponding to Eq. (10). Integrate twice to obtain

$$\overline{t}_h(\mu)=k_1H(-\mu_C,\mu)+k_2, \tag{31}$$

where

$$H(\mu_1,\mu_2)=\int_{\mu_1}^{\mu_2} e^{\beta W(\mu')}\,d\mu' \tag{32}$$

and k_1 and k_2 are constants of integration.

The particular solution $\overline{t}_p(\mu)$ is constructed from two independent solutions of the homogeneous equation. We use $y_1(\mu)=1$ and $y_2(\mu)=H(-\mu_C,\mu)$. The Wronskian is $\mathcal{W}=\exp[\beta W(\mu)]$. Using the variation of parameters formula yields

$$\overline{t}_p(\mu)=\frac{1}{\mathcal{D}}\int_{-\mu_C}^{\mu} e^{-\beta W(\mu')}\times[H(-\mu_C,\mu')-H(-\mu_C,\mu)]d\mu'. \tag{33}$$

The general solution is then $\overline{t}(\mu)=\overline{t}_h(\mu)+\overline{t}_p(\mu)$. Applying the boundary conditions Eqs. (27) and (30) and simplifying finally gives an expression for the mean first passage time using the LSA:

$$\begin{aligned}\mathcal{D}\overline{t}_{\mathrm{LSA}}(\mu)=&H(-\mu_C,\mu_C)G(-\mu_C,\mu_C)\\&-H(-\mu_C,\mu)G(-\mu_C,\mu)-I(-\mu_C,\mu_C)\\&+I(-\mu_C,\mu)+G(-\mu_A,-\mu_C)\\&\times[H(-\mu_C,\mu_C)-H(-\mu_C,\mu)],\end{aligned} \tag{34}$$

where we define the integrals

$$G(\mu_1,\mu_2)=\int_{\mu_1}^{\mu_2} e^{-\beta W(\mu')}\,d\mu', \tag{35}$$

$$I(\mu_1,\mu_2)=\int_{\mu_1}^{\mu_2} e^{-\beta W(\mu')}H(\mu_1,\mu')d\mu'. \tag{36}$$

Consider a diffuser initially at boundary state b_{II}. The mean first passage time to reach state b_{I} is $\bar{t}_{\mathrm{LSA}}(-\mu_C)$.

III. EXACT AND INTERIOR MEAN FIRST PASSAGE TIMES

A good characterization of the time required to cross a potential barrier by a single number is the mean first passage time for a process, beginning at a potential minimum on one side of the barrier, to reach the minimum on the other side. Therefore, we will refer to the mean first passage time for a diffuser, starting at $\mu\in[-\mu_A,\mu_{\min}]$, to reach $\mu=\mu_{\min}$ as the *exact* mean first passage time, and denote it by $\bar{t}_{\mathrm{Ex}}$. Here, $\mu_{\min}=\alpha\chi_{\min}$, with $\chi_{\min}=6.5e_0$ Å and $-\chi_{\min}$ the coordinates of the potential minima in Fig. 1(B). $\bar{t}_{\mathrm{Ex}}$ is the solution of Eqs. (10) and (30) with $\bar{t}(\mu_{\min})=\bar{t}'(-\mu_A)=0$. For $\mu\in[-\mu_A,\mu_{\min}]$:

$$\mathcal{D}\bar{t}_{\mathrm{Ex}}(\mu)=H(-\mu_A,\mu_{\min})G(-\mu_A,\mu_{\min})-I(-\mu_A,\mu_{\min})-H(-\mu_A,\mu)G(-\mu_A,\mu)+I(-\mu_A,\mu). \tag{37}$$

The interior solution $\bar{t}_{\mathrm{Int}}(\mu)$ is similar to the exact solution except that one computes the mean first time to reach μ_C instead of $\mu_{\min}$. For $\mu\in[-\mu_A,\mu_C]$:

$$\mathcal{D}\bar{t}_{\mathrm{Int}}(\mu)=H(-\mu_A,\mu_C)G(-\mu_A,\mu_C)-I(-\mu_A,\mu_C)-H(-\mu_A,\mu)G(-\mu_A,\mu)+I(-\mu_A,\mu). \tag{38}$$

A. Identity of LSA and interior times

Using the addition property of integrals with respect to their interval of integration, we can rewrite the interior solution as

$$\begin{aligned}\mathcal{D}\bar{t}_{\mathrm{Int}}(\mu)=&H(-\mu_C,\mu_C)G(-\mu_C,\mu_C)+H(-\mu_C,\mu_C)G(-\mu_A,-\mu_C)+H(-\mu_A,-\mu_C)G(-\mu_C,\mu_C)\\&+H(-\mu_A,-\mu_C)G(-\mu_A,-\mu_C)-H(-\mu_C,\mu)G(-\mu_C,\mu)-H(-\mu_C,\mu)G(-\mu_A,-\mu_C)\\&-H(-\mu_A,-\mu_C)G(-\mu_C,\mu)-H(-\mu_A,-\mu_C)G(-\mu_A,-\mu_C)-\int_{\mu}^{\mu_C}e^{-\beta W(\mu')}H(-\mu_C,\mu')d\mu'\\&-\int_{\mu}^{\mu_C}e^{-\beta W(\mu')}H(-\mu_A,-\mu_C)d\mu'.\end{aligned} \tag{39}$$

Equation (39) can be simplified in the following way. The fourth and eighth terms cancel, the third term cancels the sum of the seventh and tenth terms, and the second and sixth terms may be combined. This results in the following:

$$\begin{aligned}\mathcal{D}\bar{t}_{\mathrm{Int}}(\mu)=&H(-\mu_C,\mu_C)G(-\mu_C,\mu_C)+H(\mu,\mu_C)\\&\times G(-\mu_A,-\mu_C)-H(-\mu_C,\mu)G(-\mu_C,\mu)\\&-\int_{\mu}^{\mu_C}e^{-\beta W(\mu')}H(-\mu_C,\mu')d\mu'.\end{aligned} \tag{40}$$

Using the addition property again, we see that formulas Eqs. (34) and (40) are identical. Thus $\bar{t}_{\mathrm{LSA}}(\mu)=\bar{t}_{\mathrm{Int}}(\mu)$ for $\mu\in[-\mu_C,\mu_C]$.

In particular, the mean first passage time to diffuse from b_{II} to b_{I} in the lumped state approximation, $\bar{t}_{\mathrm{LSA}}(-\mu_C)$, is the same as the mean first passage time to diffuse from $\mu=-\mu_C$ to $\mu=\mu_C$ in the absence of the lumped state approximation, $\bar{t}_{\mathrm{Int}}(-\mu_C)$. Qualitatively, this suggests that $\bar{t}_{\mathrm{LSA}}(-\mu_C)$ gives a good approximation to $\bar{t}_{\mathrm{Ex}}(-\mu_{\min})$ when the time to cross the boundary regions can be neglected in comparison with the time to cross the pore interior.

IV. LSA WITH EFFECTIVE ELECTRICAL DISTANCE

In the proton conduction model,[1,2] the probabilities v_R and η_R are explicitly dependent on applied potential. Their expressions correspond to making the following approximations to the boundary weights a_{I} and a_{II}:

$$\tilde{a}_{\mathrm{I}}=\mathcal{L}^{-1}\int_{\mu_C}^{\mu_A}e^{-\beta\Delta\Phi(\mu)}e^{\beta f_{\mathrm{I}}\Psi_{\mathrm{I}}}d\mu, \tag{41}$$

$$\tilde{a}_{\mathrm{II}}=\mathcal{L}^{-1}\int_{-\mu_A}^{-\mu_C}e^{-\beta\Delta\Phi(\mu)}e^{-\beta f_{\mathrm{II}}\Psi_{\mathrm{I}}}d\mu. \tag{42}$$

Compare these with Eqs. (17) and (18). $\Delta\Phi(\mu)=\Phi(\mu)-\Phi(\mu_0)$ with $\mu_0=\mu_C$ on side I and $\mu_0=-\mu_C$ on side II. $\Psi_{\mathrm{I}}=e_0V_{\mathrm{I}}$, where V_{I} is the applied potential on side I. f_R, with $R\in\{\mathrm{I},\mathrm{II}\}$, is an average fraction of the applied potential drop between boundary region R and μ_0. We call f_R an effective electrical distance in analogy with the terminology of Eyring rate theory.[13] The f_R are positive; the signs of the exponents containing the f_R can be understood from the sense of the electrical potential drop Ψ shown in Fig. 1(B). Replacing $a_{\mathrm{II}}\rightarrow\tilde{a}_{\mathrm{II}}$ in Eq. (27), we obtain

$$\bar{t}'(-\mu_C)=-\mathcal{L}\tilde{a}_{\mathrm{II}}/\mathcal{D}. \tag{43}$$

The boundary condition Eq. (30) on side I remains unchanged. We refer to the solution of Eq. (10) with these

TABLE I. Comparison of mean first passage times across the molecular dynamics potential barrier shown in Fig. 1(B) using various methods. Times are in nanoseconds.

	$\chi_C=4.5e_0$ Å		$\chi_C=5.5e_0$ Å		$\chi_C=6.5e_0$ Å		$\chi_{\min}=6.5e_0$ Å	
Voltage V	EED	LSA	EED	LSA	EED	LSA	Exact	Kramers'
−0.5	53.94	55.64	57.13	58.68	58.51	59.08	59.09	58.91
−0.2	9.93	9.98	10.20	10.24	10.25	10.27	10.27	10.19
−0.1	5.87	5.88	6.01	6.01	6.02	6.02	6.03	5.97
−0.05	4.55	4.55	4.65	4.65	4.66	4.66	4.66	4.61
0	3.55	3.55	3.62	3.62	3.63	3.63	3.63	3.58
0.05	2.78	2.78	2.84	2.84	2.84	2.84	2.84	2.80
0.1	2.19	2.19	2.24	2.24	2.24	2.25	2.24	2.21
0.2	1.38	1.38	1.41	1.42	1.43	1.43	1.42	1.39
0.5	0.390	0.402	0.414	0.423	0.436	0.439	0.425	0.407

boundary conditions as $\bar{t}_{\mathrm{EED}}$, since the boundary conditions contain an effective electrical distance. The solution is

$$\begin{aligned}\mathcal{D}\bar{t}_{\mathrm{EED}}(\mu)=&H(-\mu_C,\mu_C)G(-\mu_C,\mu_C)\\&-H(-\mu_C,\mu)G(-\mu_C,\mu)-I(-\mu_C,\mu_C)\\&+I(-\mu_C,\mu)+\Theta[H(-\mu_C,\mu_C)\\&-H(-\mu_C,\mu)],\end{aligned}\tag{44}$$

where

$$\Theta=\mathcal{L}\tilde{a}_{\mathrm{II}}\exp\{-\beta W(-\mu_C)\}.\tag{45}$$

Now examine the difference between Eqs. (34) and (44):

$$\bar{t}_{\mathrm{EED}}(\mu)-\bar{t}_{\mathrm{LSA}}(\mu)=H(\mu,\mu_C)[\Theta-G(-\mu_A,-\mu_C)].\tag{46}$$

We may choose f_{II} to minimize $\bar{t}_{\mathrm{EED}}-\bar{t}_{\mathrm{LSA}}$. This difference is zero if $\Theta=G(-\mu_A,\mu_C)$, or if

$$e^{-\beta f_{\mathrm{II}}\Psi_I}=\langle e^{-\beta\Delta\Psi(\mu)}\rangle_{\mathrm{II}},\tag{47}$$

where $\Delta\Psi(\mu)=\Psi(\mu)-\Psi(-\mu_C)$ and $\langle\ldots\rangle_{\mathrm{II}}$ denotes the expected value

$$\langle A(\mu)\rangle_{\mathrm{II}}=\int_{-\mu_A}^{-\mu_C}A(\mu)e^{-\beta\Phi(\mu)}\,d\mu\Big/\int_{-\mu_A}^{-\mu_C}e^{-\beta\Phi(\mu)}\,d\mu.\tag{48}$$

Equation (47) may also be obtained by requiring that the choice of f_{II} gives $\tilde{a}_{\mathrm{II}}=a_{\mathrm{II}}$.

A difficulty with Eq. (47) is that f_{II} will, in general, depend on Ψ_{I}. For the special case of proton conduction through gramicidin, the applied electrical field in the pore is approximately constant,[10,11] and μ is the axial component of the dipole moment of the pore contents. In this case we put $\Psi(\mu)=-\mu E$, where $E=V_{\mathrm{I}}/L, V_{\mathrm{I}}$ is the applied voltage and L is the length of the pore. Then

$$\Delta\Psi(\mu)=(|\mu|-\mu_C)\Psi_{\mathrm{I}}/(e_0L),\tag{49}$$

and for small applied fields, we can expand Eq. (47) in powers of the small parameter $\beta\Psi_{\mathrm{I}}$. Hence

$$1-\beta f_{\mathrm{II}}\Psi_{\mathrm{I}}+\mathcal{O}(2)=\langle 1-\beta\Delta\Psi(\mu)+\mathcal{O}(2)\rangle_{\mathrm{II}}\tag{50}$$

or $f_{\mathrm{II}}\Psi_{\mathrm{I}}=\langle\Delta\Psi(\mu)\rangle_{\mathrm{II}}$. On side I an analogous formula may be obtained. Thus in the case of a constant electric field within the pore

$$f_{\mathrm{I}}=(\langle\mu\rangle_{\mathrm{I}}-\mu_C)/(e_0L),\tag{51}$$

$$f_{\mathrm{II}}=(|\langle\mu\rangle_{\mathrm{II}}|-\mu_C)/(e_0L).\tag{52}$$

$\langle\mu\rangle_{\mathrm{I}}$ and $\langle\mu\rangle_{\mathrm{II}}$ may be considered effective electrical coordinates of boundary regions I and II. Their values are optimal for approximating $\bar{t}_{\mathrm{LSA}}$ by $\bar{t}_{\mathrm{EED}}$ at low applied potential.

V. NUMERICAL RESULTS

In this section we compare the mean first passage times computed using the LSA Eq. (34), the exact solution Eq. (37), the interior solution Eq. (38), the effective electrical distance solution Eq. (44), and Kramers' escape theory.[3]

TABLE II. Mean first passage times across a uniformly rescaled potential barrier, with maximum height reduced from the molecular dynamics value by $4k_BT$. Times are in nanoseconds.

	$\chi_C=4.5e_0$ Å		$\chi_C=5.5e_0$ Å		$\chi_C=6.5e_0$ Å		$\chi_{\min}=6.5e_0$ Å	
Voltage V	EED	LSA	EED	LSA	EED	LSA	Exact	Kramers'
−0.5	2.705	2.840	3.382	3.484	3.805	3.841	3.841	3.666
−0.2	0.506	0.509	0.568	0.570	0.596	0.597	0.597	0.534
−0.1	0.309	0.310	0.341	0.342	0.355	0.355	0.355	0.307
−0.05	0.245	0.245	0.269	0.269	0.279	0.279	0.279	0.237
0	0.196	0.196	0.215	0.215	0.223	0.223	0.223	0.185
0.05	0.159	0.159	0.174	0.174	0.180	0.180	0.180	0.146
0.1	0.130	0.130	0.142	0.142	0.147	0.147	0.147	0.117
0.2	0.0890	0.0896	0.0986	0.0989	0.103	0.103	0.103	0.0780
0.5	0.0359	0.0370	0.0419	0.0425	0.0452	0.0454	0.0450	0.0302

Kramers' theory assumes that the diffuser attains a quasi-equilibrium state in a deep potential well before making a transit over a high barrier. The corresponding mean first passage time is

$$k^{-1}=\mathcal{D}^{-1}\int_{\mu_1}^{\mu_2}e^{\beta W(\mu)}\,d\mu\int_{\mu_3}^{\mu_4}e^{-\beta W(\mu)}\,d\mu, \tag{53}$$

where k is the crossing rate, the barrier is in the interval (μ_1,μ_2) and the potential well is in the interval (μ_3,μ_4). When the top of the barrier and the bottom of the well can be approximated by quadratic extrema, the classical rate theory expression is obtained. However, the expression in Eq. (53) may be evaluated for more general barrier and well shapes. For definiteness, we evaluate Eq. (53) with $\mu_1=-\mu_{\min}$, $\mu_2=\mu_{\min}$, $\mu_3=0$ and $\mu_4=-\mu_A$. Here, $\mu_{\min}=\alpha\chi_{\min}$, with $\chi_{\min}=6.5e_0$ Å, is the value corresponding to the potential minimum in Fig. 1(B) and $\mu_3=0$ is the value corresponding to the center of the barrier.

The LSA does not compete with Kramers' theory as a method for computing first passage times. The latter is used because of the simplicity of Eq. (53), and especially the simplicity and physical clarity of the formula obtained for the case of quadratic extrema. In contrast, the formula for the LSA, Eq. (34), is as complicated as the formula for the exact mean first passage time, Eq. (37). However, the comparison between Kramers' theory and the LSA below will emphasize the accuracy of the latter approach.

We first consider the mean first passage times to cross the molecular dynamics potential of mean force, shown in Fig. 1(B). We compare mean first passage times computed using the LSA and EED, for three different values of $\mu_C=\alpha\chi_C$, with both the exact mean first passage time and that obtained from Kramers' escape rate. We use the dipole diffusion coefficient $\mathcal{D}=\alpha^2\times 1.08(e_0\,\text{Å})^2\,\text{ps}^{-1}$, obtained from the velocity autocorrelation function of the reaction coordinate.[1] See Table I for the calculated values using each method. Relative errors of the LSA and EED mean first passage times, calculated with respect to the exact mean first passage time, are less than 1%, except for the cases of $\chi_C=4.5e_0$ Å or $V_1=\pm 0.5$ V. Relative errors of the Kramers' mean first passage time are less than 2%, except for the case $V_1=0.5$ V. We next make the same comparisons with the potential uniformly scaled so that barrier heights are reduced by $4k_BT$; see Table II. Relative errors are generally larger for the reduced barrier heights. However, for the LSA and EED cases, these are still within 1% of the exact solution for $\chi_C=6.5e_0$ Å and within 5% for $\chi_C=5.5e_0$ Å, except for $V_1=\pm 0.5$ V. Relative errors of the Kramer's estimates are poor, as expected. The magnitudes of applied voltages most commonly encountered in electrophysiology are 0.2 V or less. In these cases, the LSA and EED estimates of mean first passage times across a central barrier, computed for $\chi_C=6.5$ or $5.5e_0$ Å, are good approximations to the exact mean first passage time for the potential shown in Fig. 1(B). When the barrier height is reduced by $4k_BT$, these estimates remain good approximations when computed using $\chi_C=6.5e_0$ Å and are fair approximations when computed using $\chi_C=5.5e_0$ Å.

We finally compare the interior solution Eq. (38) with the LSA at zero applied voltage and varying χ_C between $4.5e_0$ Å and $8.1e_0$ Å. Comparisons for the molecular dynamics and rescaled barriers are shown in Table III. The numerical results agree to seven or eight decimal digits, reflecting our proof that these two quantities are the same within their common domain. For the molecular dynamics barrier, first passage times decrease by less than 1% as χ_C decreases from 8.1 to $5.3e_0$ Å. For the reduced barrier, first passage times decrease by about 10% as χ_C decreases in the same range.

VI. CONCLUSION

This paper obtains formulas for the mean first passage time to diffuse between the boundary states, using either the LSA or the EED variant. The latter assigns the boundary states an effective electrical coordinate, giving an explicit dependence of the single proton conduction model on applied electrical potential. The LSA mean first passage time is shown to be identical to an interior first passage time in their common domains. This result shows that the LSA is accurate when the time required to cross a boundary region can be neglected in comparison with the time required to cross the pore interior. Further, an optimal value is found for the electrical coordinate in the EED variant of the LSA method. Our numerical results show that the single proton model incorporating the LSA gives an accurate description of mean first passage times to cross the reorientation segment when there is a significant barrier to diffusion and the boundary regions are not too wide. For most of the cases considered, the LSA gives estimates of the mean first passage time that are more precise than those given by Kramers' theory. This is especially true when the potential barrier is low.

The LSA was introduced in order to model in a simple way proton entrance into and exit from the ion channel gramicidin. Although transport of a proton through the pore seems to be well described by a single reaction coordinate, it is necessary to take into account a range of pore water states at one end of the pore when the excess proton is just outside the channel at the other end. These potentially higher-dimensional dynamics are collapsed by the LSA. The resulting one-dimensional model can be solved analytically.

TABLE III. Comparison of LSA and Interior mean first passage times for the molecular dynamics and rescaled potential barriers. Times are in nanoseconds.

	Molecular dynamics		Reduced barrier	
χ_C	LSA	Interior	LSA	Interior
4.5	3.546 256 9	3.546 256 9	0.196 314 87	0.196 314 87
4.9	3.579 138 2	3.579 138 2	0.204 180 23	0.204 180 23
5.3	3.612 293 9	3.612 293 9	0.212 066 05	0.212 066 05
5.7	3.625 282 8	3.625 282 9	0.217 424 43	0.217 424 44
6.1	3.627 770 4	3.627 770 4	0.220 338 97	0.220 338 98
6.5	3.629 071 9	3.629 071 9	0.222 646 93	0.222 646 95
6.9	3.630 429 6	3.630 429 6	0.224 991 63	0.224 991 64
7.3	3.632 380 1	3.632 380 1	0.227 678 20	0.227 678 21
7.7	3.635 134 9	3.635 134 9	0.230 745 02	0.230 745 03
8.1	3.638 511 7	3.638 511 7	0.234 059 79	0.234 059 80

The combination of molecular dynamics and configuration space methods used to analyze proton conduction through gramicidin may become applicable to other systems as information on the structure of intermediate states becomes available. Examples for which some structural information are currently available include proton transfer in a photosynthetic reaction center,[14] a potassium channel,[15] and proton transport in bacteriorhodopsin.[16,17] It does not seem necessary that the conduction pathway be geometrically linear like gramicidin. What is required is that the dynamics can be described by a series of steps that can be parameterized using a single reaction coordinate, leading to a quasi-one-dimensional configuration space such as that shown in Fig. 1(A). It may then be the case that when protons (for example) enter the system at one end of the pathway, it is necessary to take into account that elements of the pathway at the opposite end can be in several different states. If the characteristic time required for diffusion (in configuration space) between these several states is short compared to the time required for proton transport, it may be possible to lump these states together using the LSA and thus preserve the essentially one dimensional character of the dynamics.

ACKNOWLEDGMENTS

This work was supported by National Science Foundation Grant No. MCB 9630475. We thank D. Busath for pointing out Refs. 16 and 17.

[1] M. F. Schumaker, R. Pomès, and B. Roux, Biophys. J. **76**, 2840-2857 (2000).
[2] M. F. Schumaker, R. Pomès, and B. Roux, Biophys. J. (in press).
[3] H. Risken, *The Fokker-Planck Equation*, 2nd ed. (Springer-Verlag, Berlin, 1989).
[4] A. S. Arseniev *et al.*, FEBS Lett. **186**, 168 (1985).
[5] L. K. Nicholson and T. A. Cross, Biochemistry **28**, 9379 (1989).
[6] R. Smith *et al.*, Biophys. J. **56**, 307 (1989).
[7] R. Pomès and B. Roux, Biophys. J. **71**, 19 (1996).
[8] R. Pomès and B. Roux, Biophys. J. **72**, A246 (1997).
[9] K. A. Duca and P. C. Jordan, Biophys. Chem. **65**, 123 (1997).
[10] P. C. Jordan, Biophys. J. **39**, 157 (1982).
[11] B. Roux, Biophys. J. **77**, 139 (1999).
[12] M. F. Schumaker (unpublished).
[13] B. Hille, *Ionic Channels of Excitable Membranes*, 2nd ed. (Sinauer Associates, Sunderland, 1992).
[14] L. Baciou and H. Michel, Biochemistry **34**, 7967 (1995).
[15] D. A. Doyle, J. Morais Cabral, R. A. Pfuetzner, A. Kuo, J. M. Gulbis, S. L. Cohen, B. T. Chait, and R. MacKinnon, Science **280**, 69 (1998).
[16] H. Leucke, Biochim. Biophys. Acta **1460**, 133 (2000).
[17] H. Kandori, Biochim. Biophys. Acta **1460**, 177 (2000).